JOURNAL OF CATALYSIS 113, 13–25 (1988)

Carbon Pathways in Methanation and Chain Growth during the Fischer–Tropsch Synthesis on Fe/Al_2O_3

D. M. STOCKWELL, D. BIANCHI,* AND C. O. BENNETT

*Department of Chemical Engineering, University of Connecticut, Storrs, Connecticut 06268, and *L.A. No. 231 du CNRS, Université Claude Bernard, 69622 Villeurbanne, Cedex, France*

Received July 28, 1987; revised February 8, 1988

The mechanism of methane and hydrocarbon formation from CO/H_2 mixtures on an unpromoted 10 wt% Fe/γ-Al_2O_3 catalyst was studied by labeling the feed mixture with ^{13}C or D. A reactive CH species was detected by CO/D_2 and $^{13}CO/H_2$ and found to deactivate slowly with time on stream. Only about 20% of the CH remained active after 1.5 h on stream at 285°C, producing about 86% of the synthesis products. Also present on the Fe surface were several monolayers of hydrogen-free carbon, but this species was not a poison. Bulk carburization took place, but exchange with ^{13}C on the surface was observed to be very slow, only about 3% of the overall synthesis rate, so that the bulk carbide did not participate appreciably in the synthesis. The transient incorporation of ^{13}C into methane and higher hydrocarbons suggested that the same large portion of the hydrocarbons was produced from the small active portion of the CH species. © 1988 Academic Press, Inc.

INTRODUCTION

Forty years ago, Kummer *et al.* (*1*) reported on results of experiments with $^{12}CO/H_2$ on iron and cobalt catalysts precarbided with ^{14}CO. Hydrocarbon products were oxidized to CO_2 over a hot wire filament, stabilized as a carbonate, and analyzed for ^{14}C content. Finding very little ^{14}C in the products, the authors concluded that "the greater part of the product of synthesis is formed by some process other than the reduction of [bulk or surface] carbide as an intermediate." Only about 10% of the products were formed via carbide reduction at 260°C, and 16% at 300°C (*1*). Before drawing this conclusion, however, the authors discussed at length the possible effects of surface heterogeneity. They noted that if only a small portion of the surface was active during the synthesis, the ^{14}C content of the products would be expected to drop suddenly to the isotopic content of the gas phase, even though they may have been formed by the reduction of surface carbon. Tests conducted by these workers to expose such a mechanism failed to do so, however, so that the results helped to generate interest in and support for chain growth by the enolic mechanism (*2*). Later experiments (*3–6*) with radioactive additives showed that primary alcohols could function as chain initiators and that to a slight extent, methanol could be incorporated repeatedly in chain growth as a monomer (*5*). Addition of methylene-labeled ketene (*7*) suggested that CH_2 functioned mainly as a chain initiator, and not appreciably as a monomer.

More recent evidence indicates that oxygen-free species are important in methanation and chain growth, however. Brady and Pettit (*8*) found that mixtures of CH_2N_2 and H_2 gave hydrocarbons in a distribution similar to that of the Fischer–Tropsch synthesis. When the $^{12}CH_2N_2$ was added to $^{13}CO/H_2$ mixtures, these authors reported (*9*) that the degree of chain growth increased and that the distribution of ^{13}C agreed best with the one predicted by the CH_x insertion mechanism. Results obtained on various metals by isotopic tracing with ^{13}CO have

0021-9517/88 $3.00
Copyright © 1988 by Academic Press, Inc.
All rights of reproduction in any form reserved.

also demonstrated the importance of CH_x species in chain growth (*10–16*). Mims and McCandlish (*14*) have reported results for a triply promoted iron catalyst. In the present work, we made use of the steady-state tracing (*17*) and other transient tracing techniques (*18, 12*) to study the behavior of various species on a 10% Fe/Al_2O_3 catalyst during the CO/H_2 reaction.

Among the Fischer–Tropsch metals, iron is probably the most complicated, and several factors contribute to this. Iron oxides are very stable so that completely reduced supported iron catalysts are rarely obtained, and the reduced portion of the iron often becomes more oxidized under reaction conditions (*2, 19*). Initially reduced iron catalysts also normally become carburized under reaction conditions. Although Ni and Co both form bulk carbides, these do not form under reaction conditions because the diffusion of carbon through these metals is some five orders of magnitude slower than that for iron (*20*). There is also a pronounced tendency for carbon deposition on the surface, owing to the ease of CO dissociation. Dissociative CO chemisorption has been observed at temperatures as low as 290 K (*21*). Other factors contributing to the complex behavior of iron catalysts include the variety of surface species present during reaction. Three forms of surface carbonaceous species have been detected after reaction on Fe(110) (*22*): a CH_x species probably consisting mostly of CH, a carbidic carbon species, and graphitic carbon. Only the first two of these species could readily be hydrogenated at reaction temperature (*22*). The same results were obtained in earlier work (*23, 24*) on our 10% Fe/Al_2O_3 catalyst, where a reduction in the working catalyst with H_2 gave methane in two distinct peaks. Titrations with oxygen (*24*) established the species as CH and C. Graphite was also detected by reduction at higher temperatures.

The early work of Emmett and co-workers (*1*) established that carbon in the bulk does not participate significantly in the hydrocarbon synthesis, but carburization and surface carbon deposition can have a dramatic effect on the initial synthesis rates. As was summarized by Niemantsverdriet and van der Kraan (*20*), reduced iron catalysts initially withdraw large amounts of carbon from the surface for carburization so that the synthesis rates are initially low. Iron-based catalysts initially present as oxides do not carburize though, so that the induction period is absent. For the reduced Fe/Al_2O_3 catalyst used here, the iron particles are of an intermediate size (20 nm) and moderate rates of carburization are observed (*23, 25*). The amount of carbon on the surface of the catalyst can be as much as one-half the amount in the bulk after carburization, so that in this case, the synthesis competes mostly with the mechanism for unreactive surface carbon deposition (*23, 24*). On a fused magnetite catalyst, competition with the bulk carbide formation was important (*26*).

Finally, it is important to note that good Fischer–Tropsch catalysts are normally promoted with Na, K, and other additives (*2, 19, 27*). K enhances the rate of carbon deposition (*28*) and selectivity toward higher molecular weight olefins and oxygenates (*2, 19, 27, 28*). Increased operating pressure has a similar effect (*2, 19, 27*). Because our experiments were conducted without these enhancements, our products were of a typically low molecular weight. This work has benefited however by the extensive results reported previously for this catalyst under the operating conditions used here (*23–25*).

METHODS

The 10 wt% Fe/Al_2O_3 catalyst was made by precipitation and was the same as that used earlier (*23–25*). Some of the physical properties obtained before are summarized in Table 1. Fresh samples of about 50 mg of the substrate were charged in a once-through microreactor, heated in flowing He to 275°C, held for 1 h, and then reduced in

TABLE 1

Characterization of 10% Fe/Al_2O_3 Catalyst Reduced 15 h at 460°C

Property	Method	Value	Reference
Area	BET	105 m^2/g	(23)
CO_{ads}	Static, −78°C	63 μmol CO/g	(23)
H_{ads}	Flow, Ref. (29)	68 μmol H/g	(23)
Fe diameter[a]	CO_{ads}	17.3 nm	(23)
Fe diameter[b]	H_{ads}	24.8 nm	(23)
Fe diameter	X-ray	16 nm	(23)
Fe diameter	TEM	16–20 nm	(23)
Fraction exposed[c]	CO_{ads}, −78°C	0.08	
Percentage reduction	Mössbauer	76%	(25)
Bed density		0.5 g/cc	
Particle size	Screened	0.59–1.18 mm	

[a] Corrected for percentage reduction, $1CO/2Fe_{surf}$.
[b] $1H/1Fe_{surf}$.
[c] Reduced surface iron atoms only.

H_2 at 450°C for 15 h or more as before (*23–25*). After cooling in H_2 to reaction temperature, a switch was made directly to CO/H_2. Following reaction, the catalyst was again reduced in H_2 at 450°C until no further CH_4 could be detected. The flow rates of all gases were always 30 ml/min under ambient conditions.

Product distributions and various transients were determined by combinations of gas chromatography (GC) and continuous inlet, high-resolution mass spectrometry (MS). To determine the ^{13}C content of hydrocarbons, the products were first separated by GC and individually cracked to CH_4 by hydrogenolysis in H_2, and then this labeled CH_4 was analyzed (*16*). By using a sample valve with 16 loops (VALCO), all of the required samples could be obtained during a single run. Somewhere during the course of these experiments NH_3 was inadvertently produced and adsorbed in our vacuum chamber, giving a small but significant background signal close to $^{13}CH_4^+$. Efforts to remove it failed and so we increased the instrument resolution to about 2100 during the chain growth experiments. This adjustment decreased the apparent sensitivity and gave a $^{13}CH_4^+$ peak which was not particularly flat on top. Statistical fluctuations are therefore more important in the present case than in the previous work (*16*). Experimental error would also result if the center of the $^{13}CH_4^+$ beam were to drift away from the narrow collector slit.

The reactors used here had nominal internal volumes of 0.5 or 0.75 ml, and so could produce rapid transients that did not obscure most of the kinetic processes on the iron surface. We used a shallow, wide bed to promote backmixing by diffusion (*30*) and narrow gas inlet and outlet tubing for rapid response. Simulation of the mixing curve obtained under reaction conditions showed that the reactor was gradientless, in accord with theory (*30*). The details of the simulation procedure are described elsewhere (*31*), and the experimental mixing curves may be found in a more detailed account of this research (*32*).

Transients reported here were recorded with a MINC-11 microcomputer (DEC) and instruments were calibrated against dilute mixtures of known composition. All reaction mixtures contained 10% CO and the quantities of H_2 and He required to give the stated H_2/CO ratio. Experiments were conducted at 1 atm total pressure.

It is well known that a practical process based on synthesis gas from coal gasification would involve a feed of H_2/CO on the order of 1 rather than 9. Our model catalyst suffers from exceedingly high carbon buildup for low H_2/CO ratios, and much of this carbon is in an inactive filamental form. By using 9/1 for H_2/CO, we minimize carbon buildup and maximize its average reactivity. Thus the detection of heterogeneous reactivity for a 9/1 feed is more significant than that for a 1/1 H_2/CO feed.

RESULTS

Preliminary measurements. A series of experiments was conducted to determine the effect of reaction conditions on the transient production of CH_4 after the switch $H_2 \rightarrow CO/H_2$, and on the selectivity to various products.

As was reported previously (*23, 24*),

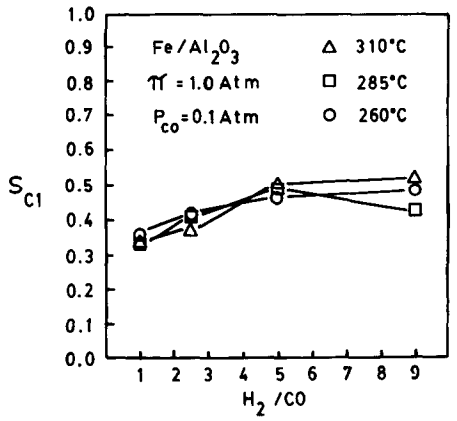

FIG. 1. Fraction of product carbon present as methane, CO_2 free, as a function of reaction conditions.

after a switch from H_2 to CO/H_2 there was initially a spike in methane production, followed by a minimum caused by the consumption of carbon for carburization and inactive surface C deposition. If a higher temperature was used, the spike was greater and the minimum more pronounced, owing to increased rates of hydrogenation and carbon accumulation (*23–25*). As carburization neared completion and graphitic carbon accumulated, the synthesis rate leveled off and then began to decline. The time scale of course depended on the temperature and H_2/CO ratio, and under the conditions used here, 20 min to 1.5 h on stream was required to reach this stage. At this point in the synthesis, chromatographic samples were taken and the product distribution was analyzed.

Figure 1 reports the efficiency of carbon conversion to methane on a CO_2-free basis. All experiments were conducted under 0.1 atm CO, varying pressures of H_2, and 1 atm total pressure. Because of the low CO pressure and the absence of promoters, the products were mostly methane. The chain growth parameter α was correspondingly small; we found values between 0.3 and 0.4 whereas values between 0.5 and 0.7 are frequently observed under more favorable conditions. The selectivity to olefins improved with decreased H_2/CO and increased temperature. The C_3 fraction contained between 35 and 95% propylene and the C_2 fraction was between 10 and 68% ethylene under the conditions of Fig. 1. Traces of acetaldehyde were also detected at the lower temperatures, but GC/MS with m/e = 31 showed that no alcohols were produced. Figure 2 indicates the nature of the oxygen-containing byproduct. For simplicity, the CO_2 rate was divided by the rate of conversion to organic carbon. When this ratio is unity at steady state, all of the byproduct oxygen is present as CO_2. Ratios in excess of unity indicate a continuing deposition of carbon. These measurements were made by methanating CO_2 in the GC/MS system and measuring the resulting methane with a flame ionization detector (FID). H_2O was not analyzed, but represents the balance in Fig. 2 at steady state.

During the stage of the synthesis at which these measurements were made, the reaction rates were in decay. If an empirical exponential poisoning law applies, time constants for the decay can be evaluated. The results are reported in Fig. 3, which shows that the most rapid decay (smallest time constant) was found at high temperatures and low H_2/CO ratios. No attempt was made to determine if any of the previ-

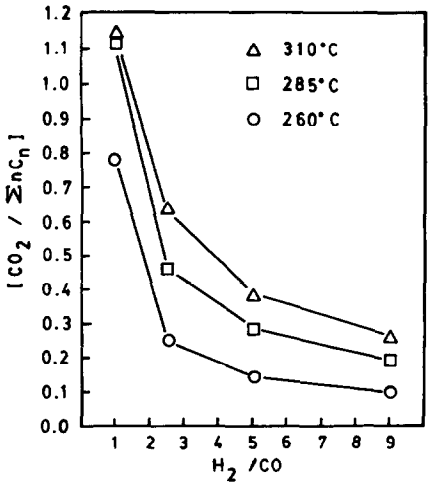

FIG. 2. Rate of CO_2 production divided by the total rate of organic carbon production (TOC). Ratios in excess of unity indicate continuing carbon deposition.

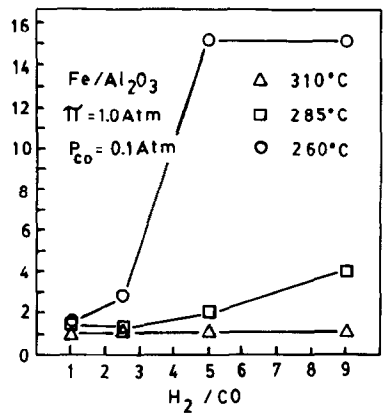

FIG. 3. Empirical deactivation times (h) observed during the experiments summarized in Figs. 1 and 2.

ous results depended substantially on the time on stream.

All of the above results are consistent with general knowledge (*2, 19, 27*) and are presented as part of the necessary characterization of this catalyst.

Titration of surface species using $^{13}CO/H_2$ and H_2. In the following experiments, we made use of the sequences $^{12}CO/He/H_2 \rightarrow {}^{13}CO/Ar/H_2$ (*11–18, 31*), and $^{12}CO/H_2 \rightarrow {}^{13}CO/H_2 \rightarrow He \rightarrow H_2$ (*12, 17, 18, 31*). Transient concentrations were followed by continuous inlet mass spectrometry.

The transient responses of ^{13}CO and Ar due to the switch $^{12}CO/He/H_2 \rightarrow {}^{13}CO/Ar/H_2$ were measured at 285°C with $H_2/CO = 9$ and 7% conversion to organic products, and found to be slightly different. The extra ^{12}CO which appeared in the reactor effluent is attributed to CO adsorbed on the iron during reaction (*11, 17, 31*). Considering the results of Kishi and Roberts (*21*), no molecular CO is expected to survive on the Fe surface, and the amount we detected was very small. Only 8 μmol CO_{ads}/g, equivalent to about 0.1 monolayer CO, was found after 1.5 h on stream.

Figure 4 shows the results obtained by the sequence $H_2 \rightarrow 30$ s $^{12}CO/H_2 \rightarrow 30$ s $^{13}CO/H_2 \rightarrow 30$ s $He \rightarrow H_2$. The H_2/CO ratio in the two reaction mixtures was 9. The transients were rapid so that we recorded the results one *m/e* peak at a time, repeating the experiment as required (*23, 24, 31*). *m/e* = 16 and 17 were used with high resolution so that the background due to H_2O was eliminated. The intensities due to hydrocarbons were negligible. The contribution of $^{13}CH_4$ to *m/e* = 16 was subtracted by the computer to give the $^{12}CH_4$ concentration, and corrections were made for the ^{12}C in the ^{13}CO. Also shown in the figure is Z_{CH_4}, which is the dimensionless, normalized atom fraction ^{13}C in the CH_4. This quantity was calculated as a function of time using the transient concentrations of $^{12}CH_4$ and $^{13}CH_4$ shown in the figure. The

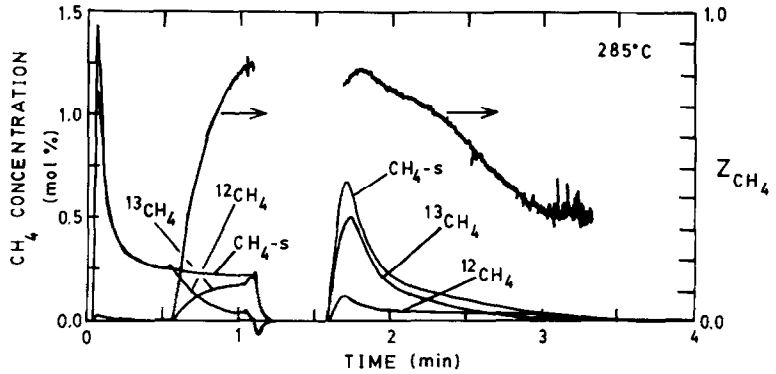

FIG. 4. $^{12}CH_4$, $^{13}CH_4$, and fraction ^{13}C in CH_4 resulting from the sequence $H_2 \rightarrow 30$ s $^{12}CO/H_2 \rightarrow 30$ s $^{13}CO/H_2 \rightarrow He \rightarrow H_2$. Also shown is the CH_4-s transient resulting from the standard experiment using only ^{12}CO.

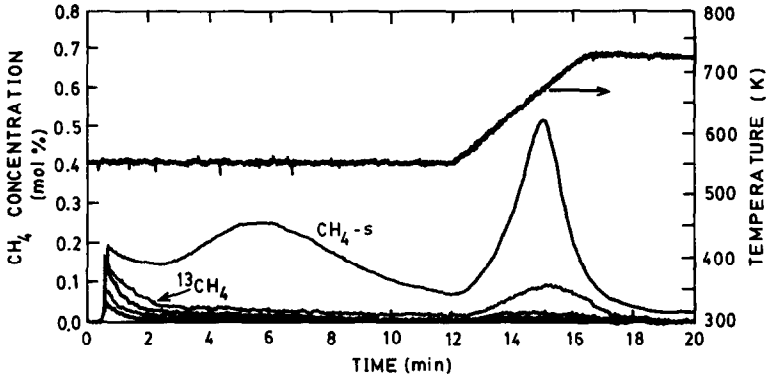

FIG. 5. Titration of the $^{13}CO/H_2$-exchanged surface with H_2 after varying times in $^{13}CO/H_2$; 1.5 h on stream at 285°C in 10% $^{12}CO/H_2$. Times in $^{13}CO/H_2$ were 25 s, 1 min, 5 min, and 30 min.

CH_4-s curve resulted when the experiment was repeated using ^{12}CO throughout.

The spike in CH_4 production after the switch $H_2 \rightarrow$ 10% CO/H_2 appears in the first few seconds of Fig. 4. In the midst of the minimum in CH_4 production, the switch to 10% $^{13}CO/H_2$ was made, $^{13}CH_4$ began to form, and the $^{12}CH_4$ concentration decayed. A switch to He and then to H_2 allowed the titration of the carbonaceous species, and we see that most of these species were converted to ^{13}C during the short exchange period. By the results obtained earlier (*23, 24*), we know that the CH species was fully established and that a small amount of the less reactive carbon had accumulated. Since only about 30 s is required to titrate the CH with H_2 at 285°C (*23*), the tail which appears after about the 2-min mark in Fig. 4 is due to the reduction of less reactive C.

At the conclusion of the $^{13}CO/H_2$ treatment, the methane was about 85% $^{13}CH_4$, and the titration of the CH with H_2 showed that the CH reduced initially was of about the same composition. Further along in the titration, however, the less reactive C is seen to have contained less ^{13}C. The lower rate of replacement with ^{13}C during reaction agrees with the longer time required to titrate the species in H_2, but C was being deposited under both $^{12}CO/H_2$ and $^{13}CO/H_2$, however, so that these results must be interpreted carefully. The next experiment will show that the less reactive C does not exchange or react under $^{13}CO/H_2$, so that the ^{13}C content of the tail in Fig. 4 was determined primarily by the amounts of C deposited under $^{12}CO/H_2$ and $^{13}CO/H_2$.

Figure 5 reports the results of the same experiment except that now we have used 1.5 h on stream in $^{12}CO/H_2$ and varied the time of reaction in $^{13}CO/H_2$. The shape of the CH_4-s produced in H_2 by the standard nonisotopic experiment has been reported for varying times on stream (*23, 24*). The initial peak is due to CH, the second peak due to less reactive C, and the subsequent tail due to the reduction of bulk carbide (*23–25*). In order to avoid long isothermal reduction times in H_2 for the carbide, the temperature was ramped at about 40 K/min to 450°C, resulting in a third peak.

As the time of exposure to $^{13}CO/H_2$ was increased, the height of the initial $^{13}CH_4$ peak increased monotonically. The less reactive C apparently did not exchange or accumulate further in $^{13}CO/H_2$. The latter result confirms the deconvolutions reported previously (*23*), which indicate that the quantity of inactive carbon begins to decrease after about 10 min on stream at 285°C. Since the reaction rates continued to decline between 1.5 and 2 h on stream, this species could not have been responsible for the deactivation (*23, 24*). After 30 min in $^{13}CO/H_2$ the bulk carbide was still only

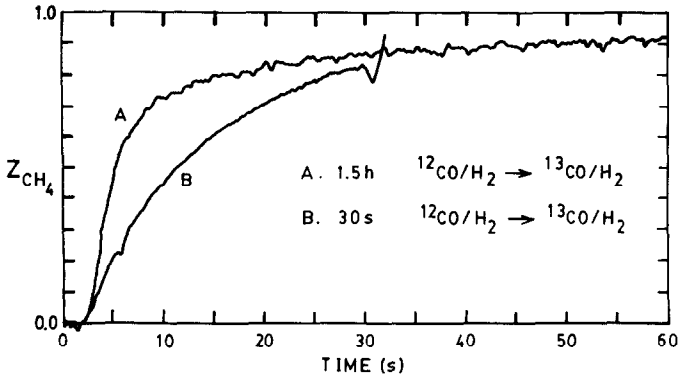

FIG. 6. Relaxation of methane to $^{13}CH_4$ after 30 s and 1.5 h on stream at 285°C and $H_2/CO = 9$. The rates of synthesis were approximately 135 and 186 μmol organic carbon/g-min after 30 s and 1.5 h on stream, respectively.

about 18% ^{13}C so that the exchange rate of bulk carbon with the surface was small. Based on homogeneous carbon pool structures (*17, 31*), we could estimate that the rate of carbon exchange with the surface was only about 3% of the synthesis rate, or about 5 μmol C/g-min. A low rate of exchange of bulk carbon is consistent with the early work of Kummer *et al.* (*1*). Although the rate of exchange of carbon with the surface was low, the rate of diffusion of carbon within the bulk is expected to be very large (*20, 25*).

It is interesting to compare the replacement of ^{12}CH with ^{13}CH in Figs. 4 and 5. After 30 s on stream (Fig. 4), 30 s in $^{13}CO/H_2$ gave CH containing 85% ^{13}C. After 1.5 h on stream (Fig. 5), 25 s in $^{13}CO/H_2$ gave CH containing only about 23% ^{13}C. After 30 min exchange, the CH was still only about 86% ^{13}C, indicating that most of the CH species reacted very slowly.

In Fig. 6 we compare the $^{13}CH_4$ transients produced under $^{13}CO/H_2$ during the previous experiments. Again, the results are reported in a normalized, dimensionless format. The definition of Z_{CH_4} is

$$Z_{CH_4} \equiv \frac{y - y_0}{y_\infty - y_0}, \qquad (1)$$

where y_0 is the fraction ^{13}C in the $^{12}CO/H_2$, y_∞ is the fraction ^{13}C in the $^{13}CO/H_2$, and y is the fraction ^{13}C in the CH_4. The initial value of Z_{CH_4} is therefore zero and the ultimate value is 1.0.

Even though the experiments were conducted under the same conditions, the relaxation of $^{13}CH_4$ was faster after 1.5 h on stream than after 30 s on stream. In fact, the response after 1.5 h on stream appears to be made up of two parts: the rapid relaxation of a small portion of the CH in Fig. 5, and a slower relaxation due to the less active CH and bulk carbide. It is significant that the small active portion of the CH seen to exchange rapidly in Fig. 5 produced most of the methane product, as shown by Fig. 6. The amount of the $^{13}CH_4$ ex ^{13}CH, the fraction ^{13}C in the CH, and the fraction ^{13}C in the CH_4 produced at the conclusion of the $^{13}CO/H_2$ treatment for the experiments of Figs. 4–6 are summarized in Table 2. Since the fraction ^{13}C in the CH and the CH_4 produced from it under $^{13}CO/H_2$ were about the same in the experiment of Fig. 4, the CH species were initially uniform in reactivity. After 1.5 h on stream in $^{12}CO/H_2$, the fraction ^{13}C in the CH during the transient under $^{13}CO/H_2$ was always less than the methane produced from it, indicating that the intermediates were nonuniform in reactivity. This is in accord with earlier results (*23, 24*) which showed that the reactivity of CH declined with time on stream. Presum-

TABLE 2

Titration of CH with $^{13}CO/H_2$ and H_2 at 285°C with $H_2/CO = 9$

Time in $^{12}CO/H_2$	Time in $^{13}CO/H_2$	Amount of $^{13}CH_4$ in H_2 (μmol/g)	Z_{CH_4} at peak maximum in H_2	Z_{CH_4} in $^{13}CO/H_2$ at maximum	X_{CO}, to organic products only
60 s	0	91[a,b]	0	0	4.7%
30 s	30 s	64[a]	0.83	0.85	
1.5 h	0	866[b]	0	0	6.9%
1.5 h	25 s	5	0.2	0.86	
1.5 h	1 min	12	0.4	0.92	
1.5 h	5 min	19	0.6	>0.95	
1.5 h	30 min	31	0.9	>0.95	

[a] Includes some less active C (*23*).
[b] No reaction in $^{13}CO/H_2$; amount of $^{12}CH_4$ under the CH_4-s curve.

ably, the deactivation of the CH is the reason for the overall loss of catalytic activity.

The results of Biloen *et al.* (*11*) for hydrocarbon synthesis over Ni, Ru, and Co catalysts at 3 atm are similar to the results reported here. In both cases, large amounts of carbon were deposited on the catalysts, with only a small fraction remaining active. Following these authors (*11*), we can estimate the quantity of the most active CH species present during the series of chain growth experiments to be discussed below. The lifetime (*11, 31*) of the active CH species is τ_{CH}. The amount of the most active portion can be obtained from the relation

$$N_{act} \approx \tau_{CH} R_{CH} \approx \tau_{CH} \sum_{n=1}^{\infty} nr_n, \qquad (2)$$

where R_{CH} is the rate of consumption of CH, which we assume was the total synthesis rate. τ_{CH} was estimated from the initial slope (*31*) of Z_{CH_4}, with the mixing time subtracted to compensate for the response of the instrumentation. The results collected in Table 3 indicate that the amount of active CH present during reaction is usually less than about 10 μmol/g after a significant time on stream. The total amount of CH present at 285°C with $H_2/CO = 9$ is about 50 μmol/g, and this quantity is apparently independent of time on stream (*23*). CO chemisorption at −78°C suggests that about 126 μmol/g of exposed iron atoms is present on the clean catalyst (*23*).

Titration of surface species using CO/D₂. With H_2/CO and $D_2/CO = 9$ at 285°C, we made a switch from $^{12}CO/H_2$ to $^{12}CO/D_2$ and observed the H_2, HD, D_2, and CD_4 transients. Experiments were conducted after 30 s and 1.5 h on stream. Owing to the complexity of the cracking patterns of the partially deuterated methanes, we did not attempt to measure the other products. High resolution allowed us to exclude any D_2O formed.

The mixing time of the reactor was 0.63 s. During the mixing transient between CO/H_2 and CO/D_2, a spike in HD was observed and attributed to scrambling of H_2 and D_2. Following the spike was a tail of HD, which we attribute to a slower exchange with the support and possibly also to the scrambling of CH_x hydrogen. The relaxation of the methane products toward pure CD_4 was similar to the relaxation toward $^{13}CH_4$ in Fig. 6. This indicates the existence of some CH_x ($x = 1$–3) species. Previous titrations of this species with oxygen (*24*) established the species as CH, and for simplicity, we have used this notation throughout.

Figure 7 makes a comparison between these results using the dimensionless format. The original concentration transients may be found elsewhere (*32*). Z_D is the atom fraction deuterium in the H_2 + HD + D_2 mixture. We did not have a calibration

TABLE 3

Amounts of the Most Active CH by the Initial Slope of Z_{CH_4}

Run No.:	1	2	3	4	5	6
Temp. (°C)	285	260	310	310	260	310
H_2/CO	9	9	9	2.5	2.5	2.5
Time on stream (h)	2.0	2.0	1.25	1.0	1.17	0.33
$\sum_{n=1}^{\infty} nr_n$, (μmol/g-min)	161	156	153	7.3	33	21
X_{CO} (%)	5.6	5.4	5.3	1.0	4.5	2.9
τ_{CH} (s)	3.2	4.4	3.8	8.5	9.4	11.4
N_{act} (μmol/g)	9	11	10	1	5	4

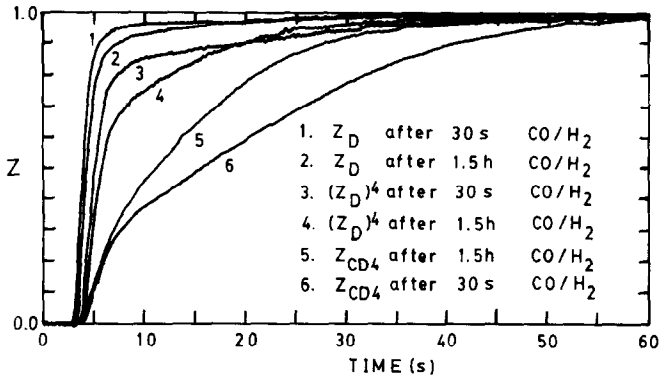

FIG. 7. Dimensionless deuterium and CD_4 transients after 30 s and 1.5 h on stream. The amounts of CH titrated by the areas between $(Z_D)^4$ and Z_{CD_4} were approximately 28 and 11 μmol CH/g for 30 s and 1.5 h on stream, respectively.

mixture for HD and the sensitivity of our instrument differed considerably between H_2 and D_2. Z_D was therefore determined from H_2 and D_2, with HD by difference. The approach of Z_D to 1.0 was rapid, except for the tail due to support exchange. If no CH_x (x = 1–3) were present, the probability of forming CD_4 from protium of composition Z_D and C would be $(Z_D)^4$, excluding isotope effects. Curves 3 and 4 are the values for $(Z_D)^4$ that we calculated from the experimental results. Z_{CD_4} is the fraction of all methanes which were CD_4. Since the intensities of the CD_4^+ signals were about constant after 1 min in CO/D_2 (*32*), an approximation to Z_{CD_4} could be obtained by normalizing the CD_4^+ signal. In making this approximation, we neglected any changes in reaction rate, any isotope effects, and any tailing effect due to slowly reacting CH_x. The assumptions combined to cause the approximation to relax more rapidly toward 1.0 than the true value of Z_{CD_4}. Curves 5 and 6 show the results obtained. Since the estimates of Z_{CD_4} relaxed more slowly than $(Z_D)^4$, there must have been some CH_x present. The areas between $(Z_D)^4$ and Z_{CD_4} represent this CH_x and the amounts found were about 28 and 11 μmol CH/g after 30 s and 1.5 h on stream. Note that the CO/D_2 experiment detects only the most active portion of the CH since the slowly reacting CH was neglected and that some of the CH hydrogen may have been scrambled away. In any event, these results are consistent in that the amount of active CH declined with time on stream.

Another important conclusion to be drawn from this experiment is that the stepwise hydrogenations $CH \rightarrow CH_2 \rightarrow CH_3 \rightarrow CH_4$ are all irreversible. Any one reversible step should have enabled the scrambling of CH_x hydrogen, in contrast to the results.

It is also interesting to note that no CH_x was detected on Ni/Al_2O_3 by the CO/D_2 (*31*) or oxygen (*33*) titrations, but that CH was detected on Ni/SiO_2 (*34*). Apparently there was little CH_x (x = 1–3) on the CCI fused magnetite catalyst (*26*). CH was the major CH_x species on Fe/TiO_2 (*35*).

Chain growth. In the remaining experiments, a switch was made from $^{12}CO/H_2$ to $^{13}CO/H_2$ and the transient incorporation of ^{13}C into methane and higher hydrocarbons was measured by GC/MS. Only the fraction ^{13}C was determined. Olefins and paraffins were lumped together. The conditions of these experiments are listed in Table 3. For runs 1, 3, and 4, the bulk iron was probably fully carburized. In the other cases, the short times on stream or the low temperature probably did not allow complete carburization (*25*). The synthesis had reached the stage where the reaction rates

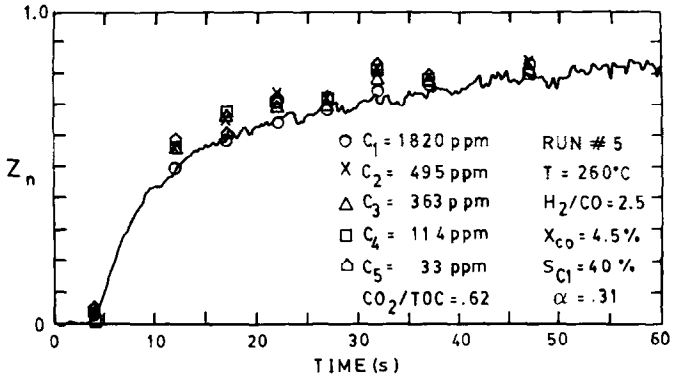

FIG. 8. Fraction ^{13}C in the synthesis products after a switch from $^{12}CO/H_2$ to $^{13}CO/H_2$ at 260°C and H_2/CO = 2.5; 70 min on stream.

had begun to decline in each experiment, however.

The results of the chain growth experiments were similar in all of the runs. Figure 8 shows the results obtained at 260°C with H_2/CO = 2.5 after 70 min on stream, a run which approached useful Fischer–Tropsch conditions. The results of the other experiments appear elsewhere (*32*). The continuous curve in Fig. 8 is the methane transient determined by mass spectrometry, just as in Fig. 6. The descrete points represent the fraction ^{13}C in methane and other hydrocarbons, as determined later by GC/MS. As discussed above, the Z_{CH_4} transient was composed of two parts: the fast response due to the active CH and the slower part due to the less active CH and exchange with bulk C. Although the division is less clear at 260°C than at the higher temperatures, only a small amount of active CH was present (Table 3). The results show that the ^{13}C content of the hydrocarbon relaxed in the same way, so that most of the hydrocarbons were probably being produced from the same small portion of the CH.

Considering the variation of any one of the Z_n from sample to sample, statistical fluctuations in the $^{13}CH_4^+$ beam current seem to have been tolerably low in this experiment. Similar fluctuations were observed in the other runs, but the relative fluctuations in run No. 4 were larger, owing to the low concentrations analyzed. The relative degree of enrichment of the various hydrocarbons also fluctuated, but the majority of the points in Fig. 8 and in the other experiments contained information on chain growth via the less active CH species and other forms of carbon. These small differences are therefore of minor significance. The best time to observe differences between the Z_n is when Z_{CH_4} is small or of intermediate value (*16*). Since this part of the Z_{CH_4} transient was so fast, none of the GC/MS samples taken corresponded to this period of time. The statistical fluctuations contained no discernible pattern and are attributed to the less satisfactory performance of the mass spectrometer at increased resolution. We believe that the basic result that the Z_n follows Z_1 is reliable, however. In summary then, the results did not depend qualitatively on the temperature or H_2/CO ratio. Apparently the most active CH species is the dominant reservoir for methanation and chain growth under all conditions in the neighborhood of 285°C and H_2/CO = 9.

DISCUSSION

Summarizing the results, we can say that great reservoirs of carbon are associated with the iron catalyst: bulk carbide, surface inactive carbon, and CH, but only a small

fraction of the CH is active for the synthesis of hydrocarbons after significant times on stream. These results are in accord with the work of Biloen *et al.* (*11*) for Ni, Co, and Ru catalysts covered with large amounts of carbon. Considering the small amounts of active species in the presence of multilayers of carbon (Ref. *11*, Tables 2 and 3, Fig. 7) it is not surprising that Kummer *et al.* (*1*) did not detect substantial incorporation of ^{14}C. Once more, previous work (*24*) on this Fe/Al_2O_3 catalyst has shown that the C deposited by $2CO \rightarrow C + CO_2$ is much different from the CH species and is probably the same as the C in the second peak of Fig. 5. As much as 309 μmol/g of this carbon can accumulate during reaction with $H_2/CO = 9$ at 285°C (*23*).

The deactivation of CH demonstrated in Fig. 5 is remarkable. It is often assumed (*22, 36*) that the cause of the deactivation is the accumulation of graphitic carbon. However, our experimental results do not indicate that the total amount of CH decreases with time on stream (*23, 24*, Fig. 5), as would be expected if portions of the surface became blocked with graphite. Instead, only the turnover frequency for many of the CH species is decreased. Our results seem to be inconsistent with the usual graphite blocking mechanism (*22, 36*).

Finally, with respect to chain growth, the Schulz–Flory–Anderson distribution model suggests that the k_p and k_t for the chain growth steps are independent of chain length. Under these circumstances the lifetimes of the growing chains, τ_n, must also be independent of n. If the τ_n were all 3–10 s like τ_{CH} (Table 3), we would have detected substantial differences between the Z_n (*16*). Since the τ_n must all be about the same, we conclude that they were all very small, and by analogy to the growing chains, that the coverage of the initiator (CH_3 for example) was also very small. Mims and McCandlish (*14*) have drawn the same conclusions from their chain growth experiments on a promoted iron catalyst and suggested that the coverages of the growing chains are 0.01 monolayer or less. Since the majority of the surface of our catalyst was covered by less active forms of carbon, the present results imply that chain growth takes place on a very localized scale. Whether or not several active CH species must be present at an active center in order for chain growth to occur is not known, but the chain growth experiments suggest that this is true. Presumably the active centers were dispersed over the surface of the catalyst and only a few active CH species were present at each one. Since the product distribution implies that chain length can increase without bound, the number of CH species at a center apparently does not restrict the chain length of products it produces. This implies of course that several of the carbon atoms in a product molecule could have come from the same site in an active center. Chain growth may even have occurred by repeated alkyl migrations between just two neighboring active CH sites. It is interesting to note that this sort of mechanism can account for the results obtained using Ni/Al_2O_3 (*16*) under conditions where the CH_x species were comparatively homogeneous and the surface relatively free of inactive carbon deposits (*31*). The agreement is encouraging and suggests that chain growth during the Fischer–Tropsch synthesis normally does occur on a very localized scale.

CONCLUSIONS

The reaction of CO and H_2 on an initially reduced Fe/Al_2O_3 catalyst leads to carburization of the bulk Fe and deposition of several monolayers of C on the surface. Neither of these species is an intermediate in the hydrocarbon synthesis. A CH species is also present and hydrocarbon synthesis takes place using carbon taken from this pool of intermediates. For short reaction times the CH species is uniform in reactivity to form hydrocarbons, but as the time on stream is increased, most of these species become deactivated. After 1.5 to 2 h on stream at 285°C with $H_2/CO = 9$, 20% of

the CH produces about 86% of the hydrocarbon products. The kinetic processes leading to CH_4 and hydrocarbon production from CH are all rapid once initiated and the coverages are therefore small.

ACKNOWLEDGMENTS

Support for this work was provided by the University of Connecticut Research Foundation and by the National Science Foundation under Grant CBT-8517158. Travel expenses were provided by the North Atlantic Treaty Organization.

REFERENCES

1. Kummer, J. T., DeWitt, T. W., and Emmett, P. H., *J. Amer. Chem. Soc.* **70,** 3632 (1948).
2. Storch, H. H., Golombic, N., and Anderson, R. B., "The Fischer–Tropsch and Related Syntheses." Wiley, New York, 1951.
3. Kummer, J. T., Spencer, W. B., Podgurski, H. H., and Emmett, P. H., *J. Amer. Chem. Soc.* **73,** 564 (1951).
4. Kummer, J. T., and Emmett, P. H., *J. Amer. Chem. Soc.* **73,** 5177 (1953).
5. Hall, W. K., Kokes, R. J., and Emmett, P. H., *J. Amer. Chem. Soc.* **79,** 2983 (1957).
6. Hall, W. K., Kokes, R. J., and Emmett, P. H., *J. Amer. Chem. Soc.* **82,** 1027 (1960).
7. Blyholder, G., and Emmett, P. H., *J. Phys. Chem.* **63,** 962 (1959).
8. Brady, R. C., and Pettit, R., *J. Amer. Chem. Soc.* **102,** 6181 (1980).
9. Brady, R. C., and Pettit, R., *J. Amer. Chem. Soc.* **103,** 1287 (1981).
10. Kobori, Y., Yamasaki, H., Naito, S., Onishi, T., and Tamaru, K., *J. Chem. Soc. Faraday Trans. 1* **78,** 1473 (1982).
11. Biloen, P., Helle, J. N., van den Berg, F. G. A., and Sachtler, W. M. H., *J. Catal.* **81,** 450 (1983).
12. Winslow, P., and Bell, A. T., *J. Catal.* **86,** 158 (1984).
13. Orita, H., Naito, S., and Tamaru, K., *J. Catal.* **90,** 183 (1984).
14. Mims, C. A., and McCandlish, L. E., *J. Amer. Chem. Soc.* **107,** 696 (1985); *J. Phys. Chem.* **91,** 929 (1987).
15. Zhang, X., and Biloen, P., *J. Catal.* **98,** 468 (1985).
16. Stockwell, D. M., and Bennett, C. O., *J. Catal.* **110,** 354 (1988).
17. Happel, J., Suzuki, I., Kokayeff, P., and Fthenakis, V., *J. Catal.* **65,** 59 (1980).
18. Cant, N., and Bell, A. T., *J. Catal.* **73,** 257 (1982).
19. Anderson, R. B., *in* "Catalysis" (P. H. Emmett, Ed.), Vol. IV. Reinhold, New York, 1956.
20. Niemantsverdriet, J. W., and van der Kraan, A. M., *J. Catal.* **72,** 385 (1981).
21. Kishi, K., and Roberts, M. W., *J. Chem. Soc. Faraday Trans. 1* **71,** 1715 (1975).
22. Bonzel, H. P., and Krebs, H. J., *Surf. Sci.* **91,** 449 (1980).
23. Bianchi, D., Borcar, S., Teule-Gay, F., and Bennett, C. O., *J. Catal.* **82,** 442 (1983).
24. Bianchi, D., Tau, L. M., Borcar, S., and Bennett, C. O., *J. Catal.* **84,** 358 (1983).
25. Tau, L. M., Borcar, S., Bianchi, D., and Bennett, C. O., *J. Catal.* **87,** 36 (1984).
26. Matsumoto, H., and Bennett, C. O., *J. Catal.* **53,** 331 (1978).
27. Roper, M. *in* "Catalysis in C_1 Chemistry" (W. Keim, Ed.). Reidel, Dordrecht, 1983.
28. Bonzel, H. P., and Krebs, H. J., *Surf. Sci.* **109,** L527 (1981).
29. Amelse, J. A., Schwartz, L. H., and Butt, J. B., *J. Catal.* **72,** 95 (1981).
30. Zielinski, J., *React. Kinet. Catal. Lett.* **17,** 69 (1981).
31. Stockwell, D. M., Chung, J. S., and Bennett, C. O., *J. Catal.*, in press.
32. Stockwell, D. M., Dissertation, The University of Connecticut, University Microfilms, Ann Arbor, MI, 1987.
33. Underwood, R. P., and Bennett, C. O., *J. Catal.* **86,** 245 (1984).
34. Happel, J., Cheh, H. Y., Otarod, M., Ozawa, S., Severdia, A. J., Yoshida, T., and Fthenakis, V., *J. Catal.* **75,** 314 (1982).
35. Tau, L. M., and Bennett, C. O., *J. Catal.* **89,** 327 (1984).
36. Dwyer, D. J., and Somorjai, G. A., *J. Catal.* **52,** 291 (1978).